PAPER

Check for updates

Tailoring stability, catalytic activity and selectivity of covalent metal–organic frameworks *via* steric modification of metal nodes†

Haiyan Duan,‡[ab] Xu Chen,‡[a] Yi-Nan Yang,[a] Jianping Zhao,[a] Xiao-Chun Lin,[a] Wen-Jing Tang,[a] Qiang Gao,[c] Guo-Hong Ning ⓘ *[a] and Dan Li ⓘ *[a]

Although many efforts have been made to tune catalytic performance *via* the modification of MOF nodes including metal exchange, defect creation and metal insertion, steric tuning of MOF nodes *via* ligand modification remains challenging and unexplored. Herein, we have successfully fabricated two two-dimensional (2D) Cu(ɪ) cyclic trinuclear unit (Cu-CTU)-based MOFs with similar structures, denoted as JNM-1 and JNM-5. JNM-1 has less steric hindrance on copper open sites, while JNM-5 incorporates bulky groups enhancing steric hindrance and partial coverage on copper open sites. Due to the steric effect, JNM-5 exhibited much higher crystallinity, porosity and chemical stability, but lower catalytic activity for hydroboration reactions than JNM-1. Interestingly, JNM-5 delivered much higher substrate selectivity and chemo-selectivity for hydroboration of olefins compared to JNM-1. Owing to its high chemical stability, JNM-5 can be reused for at least five cycles without losing catalytic performance and crystallinity, while the catalytic activity of JNM-1 is greatly decreased and it turns into an amorphous material after five cycles.

10th anniversary statement

Journal of Materials Chemistry A is one of the most reputable journals for chemists in the field of materials chemistry. The development of novel metal- and covalent-organic frameworks (MOFs and COFs) with advanced functions has been a worthwhile pursuit in materials science and has grown with *Journal of Materials Chemistry A*. By combining the chemistry of MOFs and COFs, we have recently developed coinage-metal-based cyclic trinuclear unit (CTU)-based covalent metal–organic frameworks (CMOFs), which have become an emerging platform for materials development, due to their excellent features such as designable synthetic approaches, open active sites, high stability and structural periodicity. We believe that there are great opportunities in the development of advanced CTU-based CMOFs with diverse structures and advanced applications. We sincerely celebrate the 10th anniversary of *Journal of Materials Chemistry A* and would contribute further to the significant advancement of the journal.

Introduction

The discovery and exploration of catalysts with superior performance including high activity, stability and selectivity is

[a]College of Chemistry and Materials Science, Guangdong Provincial Key Laboratory of Functional Supramolecular Coordination Materials and Applications, Jinan University, Guangzhou 510632, China. E-mail: guohongning@jnu.edu.cn; danli@jnu.edu.cn

[b]International Joint Laboratory of Catalytic Chemistry, College of Sciences, Shanghai University, Shanghai 200444, China

[c]CAS Key Lab of Low-Carbon Conversion Science and Engineering, Shanghai Advanced Research Institute, Chinese Academy of Sciences, Shanghai 201210, China

† Electronic supplementary information (ESI) available: Experimental details, DFT calculations, PXRD, TGA, FTIR, solid-state NMR, SEM, EDS, TEM, XPS, catalytic kinetics, reaction mechanisms, comparison of catalytic performance, and ^1H and ^{13}C NMR spectra for new compounds. CCDC 2100102. For ESI and crystallographic data in CIF or other electronic format see DOI: https://doi.org/10.1039/d2ta08797a

‡ These authors contributed equally.

not only a fundamental challenge but also highly desired for industrial applications.[1,2] Conventionally, compared to homogeneous catalysts, heterogeneous catalysts are more often used in industrial processes because of their easy separation, excellent recyclability and high stability.[3–11] However, many traditional heterogeneous catalysts are lacking well-defined and periodic structures as well as finely tunable structural parameters; thus, their discovery usually relied on intuitive design or trial-and-error rather than hypothesis-guided, rational design and screening.[12,13]

Metal–organic frameworks (MOFs) are a class of crystalline porous materials composed of metal ions/clusters and organic linkers,[14–18] and they have been considered as promising heterogeneous catalysts due to their atomically precise and periodic structures, the presence of coordinatively unsaturated sites or open metal sites, and intrinsic porosity.[19–24] More importantly, the chemical designability and tunability of MOFs potentially allowed chemists to explore the design principle for

This journal is © The Royal Society of Chemistry 2023

J. Mater. Chem. A, 2023, 11, 12777–12783 | **12777**

tuning catalytic performance along with molecular understanding.[25–28] Specifically, the catalytic performance of MOFs can be effectively mediated at a molecular level through several strategies including the modification of metal nodes, the introduction of organic linkers with functional groups, and the encapsulation of other active species. It is well known that the modulation of steric effects on metal centres can greatly impact the catalytic activity and selectivity of homogeneous catalysts. So, it can be envisioned that the catalytic performance of MOFs can be mediated *via* the steric modification of metal nodes.

Surprisingly, although many examples have been reported for investigating the alteration of MOFs' catalytic performance *via* the modification of metal nodes such as metal exchange,[29–32] defect creation,[33–35] and metal insertion (Scheme 1a),[36–41] the steric tuning of MOF nodes *via* ligand modification is less explored. This may be because, unlike homogeneous catalysts, the modification of organic linkers usually induces the structural transformation of metal nodes and produces completely different MOF structures,[42] leading to difficulty in comparing their catalytic performance and hampering further understanding of molecular design principles.

Recently, we have prepared copper(ı) cyclic trinuclear unit (Cu-CTU)-based two-dimensional (2D) MOFs by combining the chemistry of MOFs and COFs.[43–45] These CMOFs (covalent metal–organic frameworks, constructed by metalated secondary building units and organic linkers *via* dynamic covalent bonds) possessed advanced features such as porous structures, favourable crystallinity, good stability, and satisfactory catalytic performance. Importantly, the introduction of bulky substitutes (*i.e.*, methyl groups) on Cu-CTUs still produced a 2D honeycomb structure.[41,43] We envisioned that the 2D Cu-CTU-based CMOFs would be a promising platform to investigate the relationship between steric effects of metal nodes and catalytic performance. Herein, a Cu-CTU-based CMOF, namely **JNM-5** (JNM represents Jinan material), was fabricated through an imine condensation reaction between a copper(ı) cyclic trinuclear complex (Cu-CTC, **2**) and 1,3,5-tris(4-formylphenyl)benzene (**4**) (Scheme 1b). For comparison, **JNM-1** with less steric hindrance was synthesized from Cu-CTC **1** and 1,3,5-tris(4-aminophenyl)benzene (**3**) (Scheme 1b).[43] **JNM-5** featured much higher crystallinity, stability and porosity than **JNM-1** due to the partially protected open metal sites by decorating the ligands with methyl groups. Due to the increase of steric hindrance on the metal nodes, **JNM-5** exhibited decreased catalytic activities for hydroboration reactions compared to **JNM-1**. However, **JNM-5** delivered superior substrate selectivity and chemo-selectivity, and it preferred catalyzing conjugated olefins rather than non-conjugated ones. In addition, **JNM-5** exhibited much higher cycling stability and reusability than **JNM-1**. Our work demonstrated that the chemical stability and catalytic performance of MOFs can be easily altered by the simple introduction of steric hindrance (methyl groups) on the organic linkers, which would be beneficial for the design of novel MOFs with superior catalytic performance.
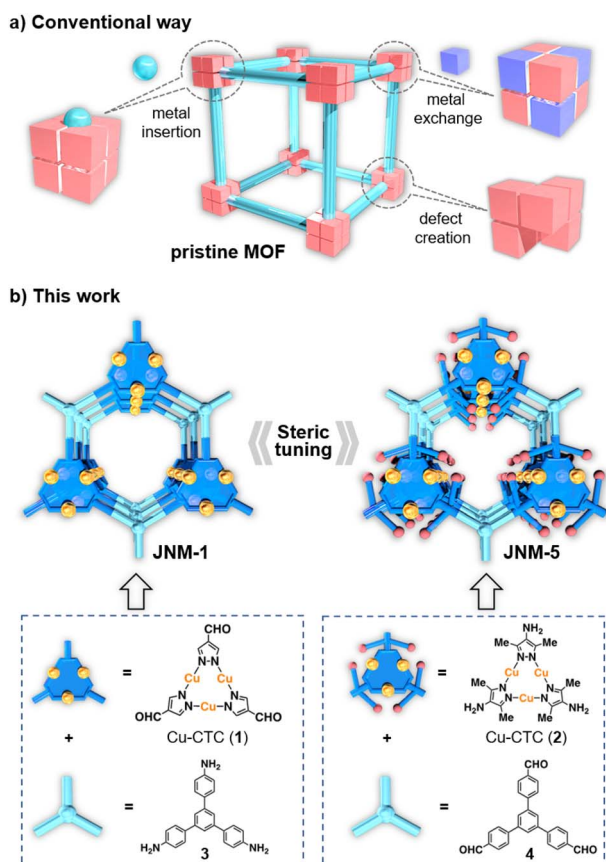

Scheme 1 Schematic illustration of (a) the conventional way for tuning the catalytic performance *via* modification of metal nodes including metal insertion, metal exchange and defect creation; (b) our work *via* steric tuning of metal nodes.

Experimental method

Synthesis of Cu-CTC (2)

A mixture of ligand 3,5-dimethyl-1*H*-pyrazol-4-amine (HL) (50.0 mg, 0.45 mmol), Cu_2O (21.5 mg, 0.15 mmol), 2 mL ethanol, and 0.2 mL pyridine were placed in an 8 mL Pyrex tube, and heated in an oven at 120 °C for 72 h. The colorless needle crystals of Cu-CTC (**2**) formed were filtered and collected under a microscope manually. The yield of Cu-CTC (**2**): 37.7 mg (72.3%, based on Cu_2O).

Synthesis of JNM-5

Cu-CTC (**2**) (26.1 mg, 0.05 mmol) and 1,3,5-tris(4-formylphenyl)benzene (**4**) (19.5 mg, 0.05 mmol) were added to a 10 mL Schlenk tube. 1,4-Dioxane (0.5 mL), mesitylene (0.5 mL), and 6 M aqueous acetic acid (0.1 mL) were added to the above mixture. Then the tube was flash frozen at 77 K in a liquid nitrogen bath and degassed with three freeze–pump–thaw cycles. After being warmed to room temperature, the mixture was heated at 120 °C for 72 h, yielding a tawny solid. The solid was separated by filtration and washed with EtOH, DMF and acetone. The resulting solid was dried under vacuum at 100 °C for 12 h. Yield: 36.3 mg (84.6%, based on **2**). Elemental analysis calc. (%): C 58.7, H 4.1, N 14.6; found: C 53.1, H 4.2, N 13.1.

12778 | *J. Mater. Chem. A*, 2023, **11**, 12777–12783

This journal is © The Royal Society of Chemistry 2023

JNM-5-catalyzed hydroboration of styrene

A solution of styrene (**5a**) (57.5 μL, 0.5 mmol), B$_2$pin$_2$ (254.2 mg, 1.0 mmol), Cs$_2$CO$_3$ (325.8 mg, 1.0 mmol), and **JNM-5** (6.4 mg, 0.0075 mmol) in CH$_3$CN (AR) (4 mL) was added to a 10 mL Pyrex tube. The mixture was stirred under a N$_2$ atmosphere for 3 h at room temperature. After the evaporation of the solvent, the crude residue was purified by flash column chromatography on silica gel (petroleum ether : ethyl acetate = 100 : 1) to afford product **6a** (107.7 mg, 0.456 mmol) in 93% yield.

Results and discussion

Cu-CTC **1** and **JNM-1** were prepared according to our reported procedures.[43] To introduce steric hindrance, Cu-CTC **2** was newly designed and synthesized from 3,5-dimethyl-1*H*-pyrazol-4-amine (Fig. S1†). The single crystal structure of **2** clearly reveals that the copper active sites are partially protected by methyl groups compared to **1** (Fig. 1a and b), giving rise to the significantly enhanced chemical and thermal stability (Fig. S2–S4†) of **2**. Afterwards, an imine condensation reaction to link **2** and organic linker **4** in a mixed solution of mesitylene, 1,4-dioxane, and 6 M aqueous acetic acid obtained highly crystal-line powders of **JNM-5** (Fig. S5†). In addition, **JNM-5** can also be obtained from Cu$_2$O, pyrazole ligand, and **4** through one-pot synthesis (Fig. S6†). Similar to **JNM-1**, the Fourier transform

Fig. 1 Crystal structure of (a) Cu-CTC (**1**) showing space-filling (left) and a stick model (right, Cu atoms shown as a ball); and (b) Cu-CTC (**2**) showing space-filling (left) and a stick model (right, Cu atoms shown as a ball) (C, H, N, O and Cu atoms are shown in cyan, white, blue, red, and orange, respectively). (c) Top (left) and side (right) views of the refined AA structure of **JNM-5**. (d) PXRD patterns of **JNM-5** (experimental curve, green line; simulated profile of AA packing mode, red line; difference plot, chartreuse line). (e) Nitrogen adsorption–desorption isotherms and the pore size distribution of JNM-5 (inset). (f) HRTEM image of **JNM-5**.

infrared (FTIR) spectrum of **JNM-5** showed CN stretching bands located at 1602 cm^{-1}, while no peaks appear at around 3382 cm^{-1} and 1690 cm^{-1} corresponding to the stretching vibrations of N–H and CO groups of starting compounds **2** and **4**, suggesting the formation of imine bonds and successful preparation of **JNM-5** (Fig. S7†). The formation of imine linkages can be further proved by characteristic resonance peaks of imine carbons at 148 ppm in solid-state ^{13}C CP/MAS NMR (Fig. S8†). The scanning electron microscopy (SEM) images taken on the surface verified that the as-formed **JNM-5** presents well-developed particle-like morphology (Fig. S9†). The uniform distribution of elements C, Cu and N was also demonstrated by energy dispersive X-ray spectroscopy (EDS) (Fig. S10†).

The crystal structure of **JNM-5** was determined by powder X-ray diffraction (PXRD) analysis (Fig. 1d). The PXRD pattern of **JNM-5** show reflections at 4.29, 7.48, 8.69, 11.45, and 26.16° corresponding to the diffractions of (100), (110), (200), (210) and (001), respectively. In addition, the structure simulation and geometry optimization were carried out through Materials Studio (see the ESI† for details). The comparison between the experimental curve and the simulated PXRD profiles including eclipsed stacking (AA), and staggered stacking (AB and ABC) models manifests that **JNM-5** has an AA stacking mode and crystallizes in the *P*3 space group (Fig. S11–S14 and Tables S2–S4†). The Pawley refinements of **JNM-5** yield the optimized unit cell parameters ($a = b = 23.5308$ Å and $c = 3.8053$ Å) with good residual factors of $R_p = 2.83\%$ and $R_{wp} = 3.45\%$. The negligible difference plot in Fig. 1d suggests that the refined PXRD patterns are in good agreement with the experimental data. The porosity of **JNM-5** was evaluated by nitrogen adsorption–desorption measurement (Fig. 1e), which exhibited type-IV isotherms with a dominant mesoporous structure. The Brunauer–Emmett–Teller (BET) surface area is calculated to be 1027 m^2 g^{-1} (Fig. 1e). The pore size distribution calculated from nonlocal density functional theory suggests a narrow pore size distribution of ~1.89 nm (Fig. 1e, inset), which is highly consistent with the simulated values from the eclipsed AA (~1.85 nm). The much larger BET surface area of **JNM-5** than that of **JNM-1** (~534 m^2 g^{-1})[43] can be attributed to the higher crystallinity of **JNM-5**. Transmission electron microscopy (TEM) was also conducted to further investigate the structure of **JNM-5**. In high resolution TEM, the micrometer-size layered structure of **JNM-5** (Fig. S15†) with a lattice spacing of 2.04 nm can be observed (Fig. 1f), which was assigned to the (100) atomic plane, further verifying the eclipsed AA stacking mode. These results unambiguously revealed that **JNM-5** features a similar 2D honeycomb structure to that of **JNM-1**, which allowed us to further study and compare their catalytic performance.

Thermal gravimetric analyses (TGA) and various temperature PXRD patterns under a N$_2$ atmosphere were both performed to probe the stability of **JNM-5**. **JNM-5** clearly demonstrated higher stability up to 390 °C than **JNM-1** (Fig. 2a and b).[43] It is also worth noting that **JNM-5** has better crystallinity under the same synthesis conditions (Fig. S16†) compared with **JNM-1**. In addition, when being exposed to air for six months and to boiling water for 1 month (Fig. S17 and S18†), the PXRD patterns of **JNM-5** did not show noticeable changes, suggesting
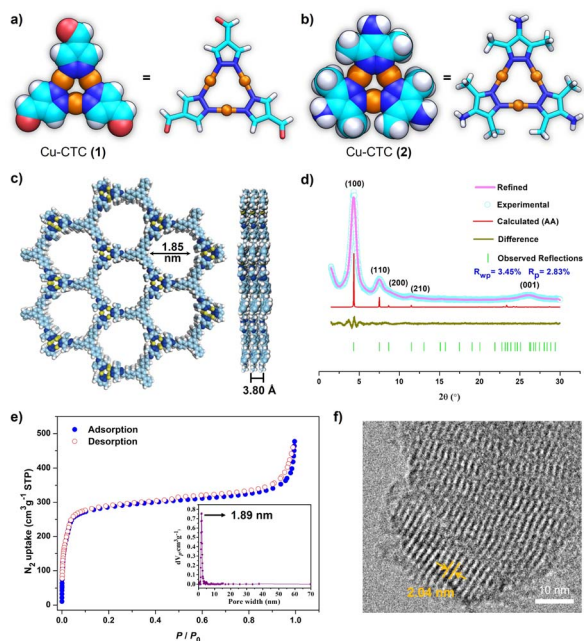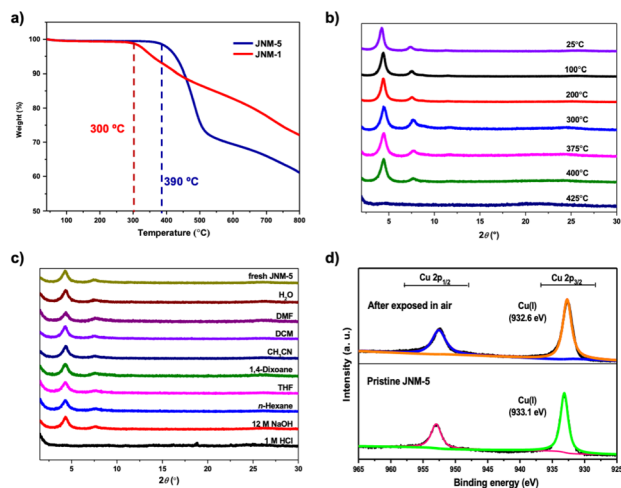
Fig. 2 (a) TGA curves of **JNM-5** and **JNM-1** (ref. 43) under a N$_2$ atmosphere. (b) *In situ* variable-temperature PXRD patterns of **JNM-5** under a N$_2$ atmosphere. (c) PXRD patterns of **JNM-5** after treatment with different solvents for 3 days. (d) XPS spectra of **JNM-5** before and after exposing to air for one month.

high robustness and chemical stability of **JNM-5**. In contrast, the crystallinity of **JNM-1** almost vanished after only 7 days in boiling water (Fig. S19†). X-ray photoelectron spectroscopy of **JNM-5** showed an intense sharp and symmetrical Cu(I) 2p$_{3/2}$ peak at 933.1 eV, indicating that only Cu(I) was found in **JNM-5**. These features remained unchanged after being exposed to air or immersed in boiling water for one month (Fig. 2d and S20†). Furthermore, **JNM-5** exhibited comparable chemical stability with **JNM-1** toward various organic solvents, water, and even 12 M NaOH solution for 3 days, while it was unstable in 1 M HCl solution (Fig. 2c). These results illustrated that the thermal and chemical stability can be largely enhanced by the tuning of steric effects on the MOF nodes.

With similar structures but differing steric hindrance on copper nodes, the catalytic performance including activity and selectivity of **JNM-1** and **JNM-5** were investigated and compared. In our previous work, **JNM-1** delivered excellent catalytic activity for the Sonogashira cross-coupling reaction.[40] However, the cross-coupling reaction of phenylacetylene and iodobenzene catalyzed by **JNM-5** produced 1,2-diphenylethyne as the coupling product with only 52% conversion under the same reaction condition (Fig. S21†). Such a lower catalytic activity of **JNM-5** than **JNM-1** (~99% conversion) can be attributed to the steric hindrance on the copper nodes, which hampered the formation of copper(I) vinyl intermediates.

The transition metal-catalyzed hydroboration of olefins is a versatile and straightforward method to access functionalized organoboron compounds, and the resulting alkylboronates are versatile intermediates for a wide range of applications in organic synthesis.[46,47] **JNM-1** and **JNM-5** were employed to test the catalytic performance of hydroboration of olefins. Initially, the hydroboration of styrene (**5a**) was chosen as the model reaction for optimizing the reaction conditions. As presented in Table 1, the hydroborylation of styrene (**5a**) and B$_2$pin$_2$ can be achieved in 93% isolated yield and >99 : 1 regioselectivity at room temperature (rt) with 1.5 mol% **JNM-5** as the catalyst and Cs$_2$CO$_3$ as the base (Table 1, entry 1), which is slightly lower than that of **JNM-1** (Table 1, entry 15). The indispensable role of **JNM-5** or Cs$_2$CO$_3$ was strongly verified by the control experiments, which did not show any hydroboration products in the absence of **JNM-5** or Cs$_2$CO$_3$ (Table 1, entries 2 and 3). The alteration of Cs$_2$CO$_3$ into triethylamine, *t*-BuOK or Na$_2$CO$_3$ led to lower yields and decreased regioselectivities (Table 1, entries 4–6). The exploration of solvent effects demonstrated that acetonitrile is the most favorable solvent for achieving high catalytic performance compared to other solvents including CH$_3$CN/H$_2$O (9 : 1), 1,4-dioxane and DMF (Table 1, entries 7–9). Decreasing the catalyst loading to 1.0 mol% resulted in lower yield (Table 1, entry 10). Increasing the catalyst loading to 2.5 mol% gave products in 99% yield and >99 : 1 regioselectivity (Table 1, entry 11). When Cu$_2$O, Cu-CTC (**1**), Cu-CTC (**2**) or organic linker (**4**) were used as catalysts instead of **JNM-5**, low yields of 41%, 12%, 81% or <1% were observed (Table 1, entries 12–14 and Fig. S22†). In addition, the gram-scale experiments under the same reaction conditions were conducted. Specifically, 1.15 g of **6a** can be eventually obtained in 82% isolated yield (Table 1, entry 16 and Fig. S23†), and the TOF was estimated to be 394 h^{-1} (Table S5†). The catalytic kinetics of **JNM-1** and **JNM-5** were estimated by the plot of conversion *versus* reaction time. In the case of **JNM-1**, product **6a** was detected at 5 min with 21% conversion, which further elevated to 95% at 45 min (Fig. S24†), while **JNM-5** required a longer reaction time to complete the reaction (Fig. S25†). Initial rate experiments

Table 1 Condition optimization of JNM-5-catalyzed hydroboration of styrene^a

Entry	Change from the "standard conditions"	Yield^b (%)	6a : 7a^b
1	None	96 (93)^c	>99 : 1
2	No **JNM-5**	<1	—
3	No Cs$_2$CO$_3$	<1	—
4	Et$_3$N, instead of Cs$_2$CO$_3$	Trace	—
5	*t*-BuOK, instead of Cs$_2$CO$_3$	44	86 : 14
6	Na$_2$CO$_3$, instead of Cs$_2$CO$_3$	64	90 : 10
7	CH$_3$CN/H$_2$O (9 : 1), instead of CH$_3$CN	84	90 : 10
8	1,4-Dioxane, instead of CH$_3$CN	60	>99 : 1
9	DMF, instead of CH$_3$CN	87	>99 : 1
10	1.0 mol% **JNM-5**	76	>99 : 1
11	2.5 mol% **JNM-5**	99	>99 : 1
12	Cu$_2$O, instead of **JNM-5**	41	>99 : 1
13	**2**, instead of **JNM-5**	81	>99 : 1
14	**4**, instead of **JNM-5**	<1	—
15	**JNM-1**, instead of **JNM-5**	99	>99 : 1
16	1.15 g scale	82^c	>99 : 1

^{a} Reaction conditions: **5a** (1.0 equiv.), B$_2$pin$_2$ (2 equiv.), Cs$_2$CO$_3$ (2 equiv.), **JNM-5** (1.5 mol%), CH$_3$CN (4 mL), room temperature (rt), N$_2$. ^{b} Determined by GC-MS analysis of the reaction mixture. ^{c} Isolated yields.

indicated that the hydroboration reaction was the first order for both **5a** and B_2pin_2. The measurement of rate constants resulted in $k_{JNM-1}/k_{JNM-5} = 2.67$ (Fig. S24 and S25†), suggesting that the introduction of a methyl group on the Cu center decreased catalytic activity for hydroboration of styrene.

Stability and recyclability are other key factors for heterogeneous catalysts; thus, we examine the crystallinity and structural integrity of **JNM-1** and **JNM-5** after catalytic cycling. Interestingly, the PXRD pattern of recovered **JNM-5** remained almost identical to the original one (Fig. 3b), and the reaction conversion slightly decreased from 97% to 90% after five catalytic cycles (Fig. 3a). In sharp contrast, **JNM-1** turned into a completely amorphous structure (Fig. 3b) and the reaction conversion largely decreased from 98% to 82% after five cycles (Fig. 3a). In addition, the XPS spectra of **JNM-5** revealed an unchanged Cu(I) $2p_{3/2}$ signal at 932.7 eV, the same as the original one, which verified the retrievable Cu(I) during recycling experiments (Fig. S26†). The Cu(II) $2p_{3/2}$ located at 934.1 eV was found in the XPS spectra of **JNM-1** after the recyclability tests, which further confirmed the instability of **JNM-1** during catalytic cycles (Fig. S27†). Based on our previous work[47] and other reported examples, a reaction mechanism was also proposed, as shown in Fig. S28.†

With the optimized conditions in hand, we explored the substrate scope for **JNM-5**-catalyzed hydroboration of olefins. As depicted in Table 2, aryl olefins possessing electron-withdrawing groups and electron-donating substituents could proceed with excellent yields (**6b–6m**). Moreover, the yield of aryl olefins with multiple electron-withdrawing groups and electron-donating substituents can also reach 85% (**6n**) and 91% (**6o**) respectively. The aryl olefins with heterocycles also achieved good yields, ranging from 79% (**6p**) to 90% (**6q**). These results confirmed that a variety of functional groups, despite their different substitution patterns and electronic properties, were all well tolerated, suggesting that **JNM-5** is an excellent heterogeneous catalyst for hydroboration of aryl olefins.

During the expansion of substrate scope, we found that olefins including naphthalene and biphenyl can both present a high yield of 94% (**6r**) and 95% (**6s**). However, a non-conjugated olefin, allylbenzene (**6t**), delivered a very low yield of 21%. Such results promoted us to further study the selectivity using **JNM-5** as the catalyst. Initially, the k_{5a}/k_{5t} ratio estimated to be 11.4 by using the plot of reaction time *versus* conversion (Fig. S25 and S29†) indicates a remarkable decrease in the reaction

Table 2 Scope of the hydroboration of olefins[a]

[a] Reaction condition: 0.5 mmol scale. [b] Isolated yields. [c] Determined by GC-MS analysis of the reaction mixture.

rate with a non-conjugated olefin and potential high substrate selectivity between the conjugated olefin and non-conjugated one. A competition experiment was conducted to reveal clearer results: when a 1 : 1 mixture of **5a** and **5t** was catalyzed with **JNM-5** (Fig. 4a), hydroboration product **6t** did not form before 90 min, resulting in excellent substrate selectivity for **5a** (**6a/6t** = 95/trace) (Fig. 4a, S30 and Table S6†). In contrast, **JNM-1**
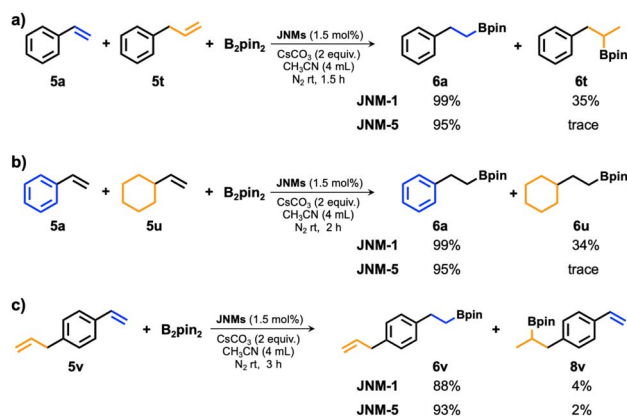

Fig. 4 Competition experiment of JNM-catalyzed hydroboration: (a) reaction conditions: **5a** (0.25 mmol), **5t** (0.25 mmol), B_2pin_2 (1 mmol), 90 min; (b) reaction conditions: **5a** (0.25 mmol), **5u** (0.25 mmol), B_2pin_2 (1 mmol), 2 hours. (c) The chemo-selectivity of JNM-catalyzed hydroboration. Reaction conditions: **5a** (1 equiv.), B_2pin_2 (2 equiv.), 3 hours. All conversions are determined by GC-MS analysis of the reaction mixture.
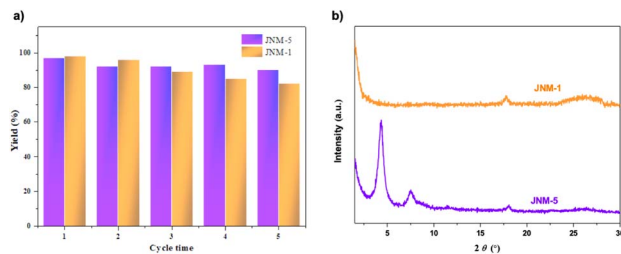

Fig. 3 (a) Recyclability of JNM-catalyzed hydroboration of styrene. The reported yield is based on GC-MS analysis. (b) PXRD for JNMs after five catalytic cycles.

This journal is © The Royal Society of Chemistry 2023

J. Mater. Chem. A, 2023, **11**, 12777–12783 | **12781**

exhibited much lower selectivity, which led to a 99/35 mixture of **6a/6t** under the same reaction conditions (Fig. 4a). In addition, we further verified substrate selectivity for a 1 : 1 mixture of **5a** and non-conjugated olefin, ethenyl-cyclohexan (**5u**), using JNMs as catalysts. As shown in Fig. 4b and S31,† the products **6a** and **6u** can be obtained in a conversion of 95% and trace at 120 min catalyzed by **JNM-5**, respectively. In the same reaction time, a **6a/6u** ratio of 99/34 can obtained using **JNM-1** as the catalyst (Fig. 4b), indicating a much lower substrate selectivity compared to that of **JNM-5**. These results revealed that although **JNM-5** exhibited lower catalytic activity, it delivered much higher substrate selectivity compared to **JNM-1**, further confirming that the steric tuning of MOF nodes could largely control their catalytic performance.

To further explore the chemo-selectivity of olefins, 1-allyl-4-vinylbenzene (**5v**) containing conjugated and non-conjugated olefins have been prepared (Fig. 4c). When **JNM-5** was employed as the catalyst, the corresponding product **6v** with a yield of 93% was obtained. More importantly, a conversion ratio between **6v** and **8v** of 46.5 : 1 suggests that **JNM-5** exhibited excellent chemo-selectivity for conjugated olefins. In sharp contrast, under the same reaction conditions, the yield of **6v** is 88% and conversion ratio between **6v** and **8v** is 22/1 using **JNM-1** as the catalyst. These results suggest that the chemo-selectivity for conjugated olefins using **JNM-5** as the catalyst is twice higher than that of **JNM-1**.

Conclusions

In summary, we have prepared two 2D Cu-CTU-based CMOFs, denoted as **JNM-1** and **JNM-5**, through imine condensation reactions. Although they have similar 2D honeycomb structures, **JNM-5** features larger steric hindrance on open copper sites than **JNM-1** due to the introduction of methyl groups on Cu-CTC. Interestingly, owing to the partially protected metal nodes, **JNM-5** featured much higher crystallinity, stability and porosity than **JNM-1**. In addition, **JNM-5** exhibited decreased catalytic activities for hydroboration reactions compared to **JNM-1**, because of steric effects. Unexpectedly, **JNM-5** delivered superior substrate selectivity and chemo-selectivity for hydroboration of conjugated aryl olefins than **JNM-1**. Owing to its high chemical stability, **JNM-5** can be reused at least for five cycles without losing catalytic performance and crystallinity, while the catalytic activity of **JNM-1** greatly decreased and it turned into an amorphous material after five cycles. Our work provides further understanding for designing heterogeneous catalysts at a molecular level and paves a novel way to rationally tune the catalytic performance of MOFs.

Conflicts of interest

There are no conflicts to declare.

Acknowledgements

References

1 C. Adams, *Top. Catal.*, 2009, **52**, 924–934.

2 R. Breslow, *Acc. Chem. Res.*, 1995, **28**, 146–153.

3 C. M. Friend and B. Xu, *Acc. Chem. Res.*, 2017, **50**, 517–521.

4 J. M. Thomas, *Angew. Chem., Int. Ed.*, 1988, **27**, 1673–1691.

5 T. W. Van Deelen, C. H. Mejía and K. P. De Jong, *Nat. Catal.*, 2019, **2**, 955–970.

6 M. J. Climent, A. Corma and S. Iborra, *Chem. Rev.*, 2011, **111**, 1072–1133.

7 A. Iemhoff, M. Vennewald and R. Palkovits, *Angew. Chem., Int. Ed.*, 2022, e202212015.

8 K. Ralphs, C. Hardacre and S. L. James, *Chem. Soc. Rev.*, 2013, **42**, 7701–7718.

9 Z. Xiao, Y. Zhou, X. Xin, Q. Zhang, L. Zhang, R. Wang and D. Sun, *Macromol. Chem. Phys.*, 2016, **217**, 599–604.

10 W. Ji, T. X. Wang, X. Ding, S. Lei and B. H. Han, *Coord. Chem. Rev.*, 2021, **439**, 213875–213904.

11 Y. M. Wang, X. C. Lin, K. M. Mo, M. Xie, Y. L. Huang, G. H. Ning and D. Li, *Angew. Chem., Int. Ed.*, 2023, e202218369.

12 F. Zaera, *Chem. Rev.*, 2022, **122**, 8594–8757.

13 J. Greeley, *Annu. Rev. Chem. Biomol. Eng.*, 2016, **7**, 605–635.

14 M. Ding, X. Cai and H.-L. Jiang, *Chem. Sci.*, 2019, **10**, 10209–10230.

15 J. R. Long and O. M. Yaghi, *Chem. Soc. Rev.*, 2009, **38**, 1213–1214.

16 H. Furukawa, K. E. Cordova, M. O'Keeffe and O. M. Yaghi, *Science*, 2013, **341**, 1230444.

17 O. M. Yaghi, M. O'Keeffe, N. W. Ockwig, H. K. Chae, M. Eddaoudi and J. Kim, *Nature*, 2003, **423**, 705–714.

18 S. Kitagawa, *Chem. Soc. Rev.*, 2014, **43**, 5415–5418.

19 L. Zhu, X.-Q. Liu, H.-L. Jiang and L.-B. Sun, *Chem. Rev.*, 2017, **117**, 8129–8176.

20 F. L. i Xamena, A. Abad, A. Corma and H. Garcia, *J. Catal.*, 2007, **250**, 294–298.

21 Q. Wang and D. Astruc, *Chem. Rev.*, 2019, **120**, 1438–1511.

22 J. Lee, O. K. Farha, J. Roberts, K. A. Scheidt, S. T. Nguyen and J. T. Hupp, *Chem. Soc. Rev.*, 2009, **38**, 1450–1459.

23 W. Tu, Y. Xu, S. Yin and R. Xu, *Adv. Mater.*, 2018, **30**, 1707582.

24 J. Luo, X. Luo, M. Xie, H. Z. Li, H. Y. Duan, H. G. Zhou, R. J. Wei, G. H. Ning and D. Li, *Nat. Commun.*, 2022, **13**, 7771–7780.

25 A. Bavykina, N. Kolobov, I. S. Khan, J. A. Bau, A. Ramirez and J. Gascon, *Chem. Rev.*, 2020, **120**, 8468–8535.

26 Z. H. Syed, F. Sha, X. Zhang, D. M. Kaphan, M. Delferro and O. K. Farha, *ACS Catal.*, 2020, **10**, 11556–11566.

27 T. A. Goetjen, J. Liu, Y. Wu, J. Sui, X. Zhang, J. T. Hupp and O. K. Farha, *Chem. Commun.*, 2020, **56**, 10409–10418.

12782 | *J. Mater. Chem. A*, 2023, **11**, 12777–12783

This journal is © The Royal Society of Chemistry 2023

28 J. Liu, L. Chen, H. Cui, J. Zhang, L. Zhang and C.-Y. Su, *Chem. Soc. Rev.*, 2014, **43**, 6011–6061.

29 S. Horike, M. Dinca, K. Tamaki and J. R. Long, *J. Am. Chem. Soc.*, 2008, **130**, 5854–5855.

30 L. Alaerts, E. Séguin, H. Poelman, F. Thibault-Starzyk, P. A. Jacobs and D. E. De Vos, *Eur. J. Chem.*, 2006, **12**, 7353–7363.

31 X. M. Lin, T. T. Li, Y. W. Wang, L. Zhang and C. Y. Su, *Chem.– Asian J.*, 2012, **7**, 2796–2804.

32 M. Y. Masoomi, A. Morsali, A. Dhakshinamoorthy and H. Garcia, *Angew. Chem., Int. Ed.*, 2019, **131**, 15330–15347.

33 S. S.-Y. Chui, S. M.-F. Lo, J. P. Charmant, A. G. Orpen and I. D. Williams, *Science*, 1999, **283**, 1148–1150.

34 A. Corma, H. Garcia and F. L. i Xamena, *Chem. Rev.*, 2010, **110**, 4606–4655.

35 S. Dissegna, K. Epp, W. R. Heinz, G. Kieslich and R. A. Fischer, *Adv. Mater.*, 2018, **30**, 1704501.

36 B. Li, J. G. Ma and P. Cheng, *Small*, 2019, **15**, 1804849.

37 Q. Yang, Q. Xu and H.-L. Jiang, *Chem. Soc. Rev.*, 2017, **46**, 4774–4808.

38 L. Cheng, Q. Guo, K. Zhao, Y.-M. Li, H. Ren, C.-Y. Ji and W. Li, *Catal. Lett.*, 2022, **185**, 1–12.

39 I. Gumus, A. Ruzgar, Y. Karatas and M. Gülcan, *Mol. Catal.*, 2021, **501**, 111363.

40 P. Y. You, R. J. Wei, G. H. Ning and D. Li, *Chem. Res. Chin. Univ.*, 2022, **38**, 415–420.

41 Y.-Z. Chen, Y.-X. Zhou, H. Wang, J. Lu, T. Uchida, Q. Xu, S.-H. Yu and H.-L. Jiang, *ACS Catal.*, 2015, **5**, 2062–2069.

42 W. Lu, Z. Wei, Z.-Y. Gu, T.-F. Liu, J. Park, J. Park, J. Tian, M. Zhang, Q. Zhang and T. Gentle III, *Chem. Soc. Rev.*, 2014, **43**, 5561–5593.

43 R. J. Wei, H. G. Zhou, Z. Y. Zhang, G. H. Ning and D. Li, *CCS Chem.*, 2020, **2**, 2045–2053.

44 H. G. Zhou, R. Q. Xia, J. Zheng, D. Q. Yuan, G. H. Ning and D. Li, *Chem. Sci.*, 2021, **12**, 6280–6286.

45 J. P. Zhao, J. Luo, Z. Lin, X. Chen, G. H. Ning, J. Liu and D. Li, *Inorg. Chem. Front.*, 2022, **9**, 4907–4912.

46 K. Burgess and M. J. Ohlmeyer, *Chem. Rev.*, 1991, **91**, 1179–1191.

47 R. J. Wei, P. Y. You, H. Y. Duan, M. Xie, R. Q. Xia, X. Chen, X. Zhao, G. H. Ning, A. I. Cooper and D. Li, *J. Am. Chem. Soc.*, 2022, **144**, 17487–17495.

This journal is © The Royal Society of Chemistry 2023

J. Mater. Chem. A, 2023, **11**, 12777–12783 | **12783**